10
Medium-assisted electromagnetic vacuum effects

The classical electromagnetic vacuum is simply the state in which all moments of the electric and induction fields identically vanish, and thus the fields themselves identically vanish. Hence, in classical electrodynamics the interaction of matter with the electromagnetic field – including field-assisted interaction between matter systems – always requires excited (source-attributed) fields, which, as is known, can be described in terms of positive semi-definite probability distribution functions in phase space. In quantum electrodynamics the situation is quite different, because the noncommutativity of canonical conjugate field quantities necessarily implies nonvanishing moments. As we know, the quantum electromagnetic vacuum can be regarded as the state in which all normally ordered field moments identically vanish. Clearly, the anti-normally ordered field moments cannot do so due to virtual photon creation and destruction – an effect in which the noise of the quantum vacuum becomes manifest.

Since the electromagnetic vacuum cannot be switched off, its interaction with atomic systems cannot be switched off either, thereby giving rise to a number of observable effects such as spontaneous emission, the Lamb shift, intermolecular energy transfer and the van der Waals force. Both virtual and real photons can be involved in the atom–field interaction. Whereas the interaction of ground-state atoms with the electromagnetic vacuum processes via virtual photon creation and destruction, the creation of real photons always requires excited atoms. A typical example of the first case is the van der Waals force between two ground-state atoms, whereas the spontaneous decay of an excited atomic state typically represents the second case.

The presence of linear media in the form of macroscopic bodies changes the structure of the electromagnetic field compared to that in the free space and in consequence the electromagnetic vacuum felt by an atom is changed. In a broader sense the effect is called the Casimir effect. It offers the possibility of controlling the interaction of atomic systems with the medium-assisted electromagnetic vacuum, with applications that range from cavity QED to integrated atom optics and electronics. On the basis of the quantization scheme for the electromagnetic field in dispersing and absorbing media (Section 2.4),

Quantum Optics, Third revised and extended edition. Werner Vogel and Dirk-Gunnar Welsch

ISBN: 3-527-40507-0

the effect of the presence of macroscopic bodies on the spontaneous emission of a single atom is studied in Section 10.1, and Section 10.2 provides a unified approach to the problem of van der Waals and Casimir forces.

10.1 Spontaneous emission

Spontaneous emission is not only one of the most familiar quantum phenomena but it is also the basic process for generating light. Although a number of properties of the spontaneously emitted radiation can be described classically, spontaneous emission is a pure quantum effect the understanding of which requires quantization of the electromagnetic field. A dynamical theory of the spontaneous emission of a single (two-level) atom in free space was first given by Weisskopf and Wigner (1930).

Let us consider a single atomic system such as an atom or a molecule – briefly referred to as an atom in the following – (position $\mathbf{r}_A$, energy eigenvalues $E_n = \hbar\omega_n$) which in the presence of arbitrary linear dielectric bodies[1] interacts with the electromagnetic field via electric-dipole transitions, so that the multipolar-coupling Hamiltonian (2.229) can be given in the form of

$$\hat{H} = \hat{H}_{\rm C} + \hat{H}_{\rm F} + \hat{H}_{\rm int}\,, \tag{10.1}$$

where

$$\hat{H}_{\rm C} = \sum_n \hbar\omega_n \hat{A}_{nn} \tag{10.2}$$

is the atomic Hamiltonian,

$$\hat{H}_{\rm F} = \int {\rm d}^3 r \int_0^\infty {\rm d}\omega\, \hbar\omega\, \hat{\mathbf{f}}^\dagger(\mathbf{r},\omega)\hat{\mathbf{f}}(\mathbf{r},\omega) \tag{10.3}$$

is the Hamiltonian of the electromagnetic field and the medium forming the bodies, and, according to Eq. (2.243),

$$\begin{aligned}\hat{H}_{\rm int} &= -\sum_{n,m} \mathbf{d}_{nm}\hat{\mathbf{E}}^{(+)}(\mathbf{r}_A)\,\hat{A}_{nm} + {\rm H.c.} \\ &= -i\sqrt{\frac{\hbar}{\pi\varepsilon_0}}\sum_{n,m}\int_0^\infty {\rm d}\omega\,\frac{\omega^2}{c^2}\int {\rm d}^3 r'\,\mathbf{d}_{nm}\boldsymbol{G}(\mathbf{r}_A,\mathbf{r}',\omega)\hat{\mathbf{f}}(\mathbf{r}',\omega)\hat{A}_{nm} + {\rm H.c.}\end{aligned} \tag{10.4}$$

1) For an extension to magnetodielectric bodies, see Ho, Buhmann, Knöll, Welsch, Scheel and Kästel (2003). It is worth noting that all formulas in this chapter which do not explicitly contain the permittivity, but are solely expressed in terms of the Green tensor (or related quantities), are also valid for magnetodielectric bodies, with the Green tensor being determined from the full Maxwell equations containing both the medium polarization and magnetization.

is the atom–field interaction energy in the electric-dipole approximation ($\hat{A}_{nm}=|n\rangle\langle m|$, $\hat{H}_{\rm C}|n\rangle=\hbar\omega_n|n\rangle$). The typical features of spontaneous decay can already be understood on the basis of a two-state model of the atom, i. e.,

$$\hat{H}_{\rm C}=\hbar\big(\omega_1\hat{A}_{11}+\omega_2\hat{A}_{22}\big)=\hbar\omega_1+\hbar\omega_{21}\hat{A}_{22}\;\mapsto\;\hat{H}_{\rm C}=\hbar\omega_{21}\hat{A}_{22} \tag{10.5}$$

($\omega_{21}=(E_2-E_1)/\hbar>0$; note that $\hat{A}_{11}+\hat{A}_{22}=1$), and within the rotating-wave approximation, i. e.,[2]

$$\hat{H}_{\rm int}=-i\sqrt{\frac{\hbar}{\pi\varepsilon_0}}\int_0^\infty {\rm d}\omega\,\frac{\omega^2}{c^2}\int {\rm d}^3r'\,\mathbf{d}_{21}\boldsymbol{G}(\mathbf{r}_A,\mathbf{r}',\omega)\hat{\mathbf{f}}(\mathbf{r}',\omega)\hat{A}_{21}+{\rm H.c.}. \tag{10.6}$$

It should be stressed that the relevant information on the bodies is fully included in the Green tensor $\boldsymbol{G}(\mathbf{r},\mathbf{r}',\omega)$ of the macroscopic Maxwell equations.

From Eq. (10.6) it is seen that when the atom is in the upper state $|2\rangle$ and the rest of the system is in the vacuum state $|\{0\}\rangle$,

$$\hat{\mathbf{f}}(\mathbf{r},\omega)|\{0\}\rangle=0, \tag{10.7}$$

then a single-quantum state of the combined field–body system,

$$|\mathbf{1}(\mathbf{r},\omega)\rangle=\hat{\mathbf{f}}^\dagger(\mathbf{r},\omega)|\{0\}\rangle, \tag{10.8}$$

can be created owing to a transition of the atom into the lower state $|1\rangle$. Hence for the overall-system state vector at time t the ansatz

$$\begin{aligned}|\psi(t)\rangle=\;&C_2(t)e^{-i\omega_{21}t}|\{0\}\rangle|2\rangle\\&+\int{\rm d}^3r\int_0^\infty{\rm d}\omega\,e^{-i\omega t}\mathbf{C}_1(\mathbf{r},\omega,t)|\mathbf{1}(\mathbf{r},\omega)\rangle|1\rangle\end{aligned} \tag{10.9}$$

can be made. To determine the (slowly varying) expansion coefficients $C_2(t)$ and $\mathbf{C}_1(\mathbf{r},\omega,t)$, we insert $|\psi(t)\rangle$ into the Schrödinger equation and obtain the following system of coupled differential equations:

$$\begin{aligned}\dot{C}_2(t)=-\frac{1}{\sqrt{\pi\varepsilon_0\hbar}}\int_0^\infty{\rm d}\omega\,\frac{\omega^2}{c^2}\,e^{-i(\omega-\omega_{21})t}\\\times\int{\rm d}^3r\,\sqrt{{\rm Im}\,\varepsilon(\mathbf{r},\omega)}\,\mathbf{d}_{21}\boldsymbol{G}(\mathbf{r}_A,\mathbf{r},\omega)\mathbf{C}_1(\mathbf{r},\omega,t),\end{aligned} \tag{10.10}$$

$$\dot{\mathbf{C}}_1(\mathbf{r},\omega,t)=\frac{1}{\sqrt{\pi\varepsilon_0\hbar}}\,\frac{\omega^2}{c^2}\,\sqrt{{\rm Im}\,\varepsilon(\mathbf{r},\omega)}\,e^{i(\omega-\omega_{21})t}\mathbf{d}_{12}\boldsymbol{G}^*(\mathbf{r}_A,\mathbf{r},\omega)\,C_2(t). \tag{10.11}$$

2) Note that here, in addition to the transverse electric field considered in Eq. (2.244), the interaction of the atom with the longitudinal electric field which is attributed to the medium is also treated in the rotating-wave approximation.

To solve it under the initial conditions $C_2(t)|_{t=0}=1$, $\mathbf{C}_1(\mathbf{r},\omega,t)|_{t=0}=0$, we formally integrate Eq. (10.11) and insert the result in Eq. (10.10). Making use of the relation (A.3), after some algebra we derive the integro-differential equation

$$\dot{C}_2(t) = \int_0^t \mathrm{d}t'\, K(t-t')C_2(t'), \tag{10.12}$$

where the kernel function reads

$$K(t) = -\frac{1}{\hbar\pi\varepsilon_0 c^2}\int_0^\infty \mathrm{d}\omega\, \omega^2 e^{-i(\omega-\omega_{21})t}\mathbf{d}_{21}\mathrm{Im}\, \boldsymbol{G}(\mathbf{r}_A,\mathbf{r}_A,\omega)\mathbf{d}_{12}\,. \tag{10.13}$$

It is not difficult to see that Eq. (10.12) can be converted into the integral equation

$$C_2(t) = \int_0^t \mathrm{d}t'\, K'(t-t')C_2(t') + 1, \tag{10.14}$$

where

$$K'(t) = \frac{1}{\hbar\pi\varepsilon_0 c^2}\int_0^\infty \mathrm{d}\omega\, \omega^2\, \frac{e^{-i(\omega-\omega_{21})t}-1}{i(\omega-\omega_{21})}\,\mathbf{d}_{21}\mathrm{Im}\, \boldsymbol{G}(\mathbf{r}_A,\mathbf{r}_A,\omega)\mathbf{d}_{12}\,. \tag{10.15}$$

Next let us calculate the intensity of the emitted radiation. From Eq. (2.295) it follows that the Heisenberg operator of the source-field part of the electric field reads

$$\hat{\mathbf{E}}_\mathrm{s}(\mathbf{r},t) = \hat{\mathbf{E}}_\mathrm{s}^{(+)}(\mathbf{r},t) + \mathrm{H.c.}, \tag{10.16}$$

where, in the rotating-wave approximation,

$$\hat{\mathbf{E}}_\mathrm{s}^{(+)}(\mathbf{r},t) = \int_0^t \mathrm{d}t'\, \boldsymbol{K}_{(E)}^{(+)}(\mathbf{r},t;\mathbf{r}_A,t')\mathbf{d}_{12}\hat{A}_{12}(t'), \tag{10.17}$$

with $\boldsymbol{K}_{(E)}^{(+)}(\mathbf{r},t;\mathbf{r}_A,t')$ being expressed in terms of the Green tensor according to Eq. (2.296).[3] Since the free-field part is in the vacuum state, the intensity of the emitted radiation is fully determined by the source-field part,

$$I(\mathbf{r},t) = \big\langle \hat{\mathbf{E}}^{(-)}(\mathbf{r},t)\hat{\mathbf{E}}^{(+)}(\mathbf{r},t)\big\rangle = \big\langle \hat{\mathbf{E}}_\mathrm{s}^{(-)}(\mathbf{r},t)\hat{\mathbf{E}}_\mathrm{s}^{(+)}(\mathbf{r},t)\big\rangle, \tag{10.18}$$

and can therefore be expressed in terms of $C_2(t)$ as

$$I(\mathbf{r},t) = \left|\int_0^t \mathrm{d}t'\, \boldsymbol{K}_{(E)}^{(+)}(\mathbf{r},t;\mathbf{r}_A,t')\mathbf{d}_{12}C_2(t')e^{-i\omega_{21}t'}\right|^2. \tag{10.19}$$

Note that only the far field contributes to the actually emitted radiation.

3) Note that for a two-level atom the polarization $\hat{\vec{P}}(\mathbf{r})$ reduces to $\hat{\vec{P}}(\mathbf{r}) = \hat{\mathbf{d}}\delta(\mathbf{r}-\mathbf{r}_A) = (\mathbf{d}_{21}\hat{A}_{21}+\mathbf{d}_{12}\hat{A}_{12})\delta(\mathbf{r}-\mathbf{r}_A)$, and that, with respect to the emitted radiation, the difference between multipolar coupling and minimal coupling becomes meaningless.

From the above it is seen that all the relevant quantities can be expressed in terms of $C_2(t)$, with the presence of macroscopic bodies being fully included in the Green tensor of the system. The calculation of $C_2(t)$ requires the solution of Eq. (10.12) [or Eq. (10.14)] – a problem, which in general must be solved numerically. However, there are two limiting cases for which Eq. (10.13) [or Eq. (10.14)] can be further evaluated analytically without explicitly making use of the actual structure of the Green tensor – namely the cases of weak and strong atom–field coupling. In the analytical calculations it may be convenient to set

$$C_2(t) = \tilde{C}_2(t) e^{-i\delta\omega_{21} t} \tag{10.20}$$

in order to determine the shifted atomic transition frequency

$$\tilde{\omega}_{21} = \omega_{21} + \delta\omega_{21} \tag{10.21}$$

in a self-consistent way. Equation (10.12) then changes to

$$\dot{\tilde{C}}_2(t) = i\delta\omega_{21}\tilde{C}_2(t) + \int_0^t \mathrm{d}t'\, \tilde{K}(t-t')\tilde{C}_2(t'), \tag{10.22}$$

where

$$\tilde{K}(t) = K(t) e^{i\delta\omega_{21} t}. \tag{10.23}$$

10.1.1 Weak atom–field coupling

We begin with the case of weak atom–field coupling, which is typical of the spontaneous emission observed, e. g., in free space. Let τ_c be the characteristic (correlation) time that defines the time interval in which $K(t)$ [Eq. (10.13)] and also $\tilde{K}(t)$ [Eq. (10.23)] are significantly different from zero. When $\tilde{C}_2(t)$ is slowly varying in this time interval, then in the time integral in Eq. (10.22) $\tilde{C}_2(t')$ may be replaced with $\tilde{C}_2(t)$ and in the remaining integral the upper limit t may be extended to infinity. In this approximation – known as the Markov approximation (cf. Section 5.1.3) – memory effects are disregarded, i. e., the temporal variation of $\tilde{C}_2(t)$ at any chosen time is solely determined by $\tilde{C}_2(t)$ at that time. In this way, the integro-differential equation (10.22) approximates to the simple differential equation

$$\dot{\tilde{C}}_2(t) = i\delta\omega_{21}\tilde{C}_2(t) + \tilde{C}_2(t) \lim_{t\to\infty} \int_0^t \mathrm{d}t'\, \tilde{K}(t-t') = -\tfrac{1}{2}\Gamma\tilde{C}_2(t), \tag{10.24}$$

leading to an exponential decay of the upper atomic state,

$$\tilde{C}_2(t) = e^{-\frac{1}{2}\Gamma t}. \tag{10.25}$$

Inserting Eq. (10.23) [together with Eq. (10.13)] in the decomposition

$$\lim_{t\to\infty}\int_0^t \mathrm{d}\tau\,\tilde{K}(\tau) = -i\delta\omega_{21} - \tfrac{1}{2}\Gamma \tag{10.26}$$

used in Eq. (10.24) and recalling the definition of the ζ function [Eq. (5.85)], we can easily see that the decay rate is given by[4]

$$\Gamma = \frac{2\tilde{\omega}_{21}^2}{\hbar\varepsilon_0 c^2}\,\mathbf{d}_{21}\mathrm{Im}\,\boldsymbol{G}(\mathbf{r}_A,\mathbf{r}_A,\tilde{\omega}_{21})\mathbf{d}_{12} \tag{10.27}$$

and for the shift of the transition frequency follows

$$\delta\omega_{21} = \frac{\mathcal{P}}{\pi\hbar\varepsilon_0 c^2}\int_0^\infty \mathrm{d}\omega\,\omega^2\,\frac{\mathbf{d}_{21}\mathrm{Im}\,\boldsymbol{G}(\mathbf{r}_A,\mathbf{r}_A,\omega)\mathbf{d}_{12}}{\tilde{\omega}_{21}-\omega}\,. \tag{10.28}$$

Note that Eq. (10.28) does not explicitly determine $\delta\omega_{21}$, because it also appears via $\tilde{\omega}_{21}$ in the frequency integral on the right-hand side of the equation. If $\delta\omega_{21}$ is set equal to zero in the frequency integral, then Eq. (10.28) becomes an explicit expression for $\delta\omega_{21}$ which is valid in lowest (nonvanishing) order of perturbation theory – an approximation widely used in practical calculations.

10.1.1.1 Decay rate and quantum yield

For an atom in free space, the Green tensor $\boldsymbol{G}(\mathbf{r},\mathbf{r}',\omega)$ reduces to the simple free-space Green tensor $\boldsymbol{G}_0(\mathbf{r},\mathbf{r}',\omega)$ given by Eq. (2.298), from which $\mathrm{Im}\,\boldsymbol{G}_0(\mathbf{r},\mathbf{r},\omega) = \boldsymbol{I}\omega/(6\pi c)$ follows, leading to the well-known formula for the spontaneous-emission rate in free space:

$$\Gamma_0 = \frac{\tilde{\omega}_{21}^3|\mathbf{d}_{21}|^2}{3\hbar\pi\varepsilon_0 c^3}\,. \tag{10.29}$$

When there are bodies in the neighborhood of the free-space region where the atom is located, then the Green tensor for the, now inhomogeneous, system can be given, in the free-space region, in the form

$$\boldsymbol{G}(\mathbf{r},\mathbf{r}',\omega) = \boldsymbol{G}_0(\mathbf{r},\mathbf{r}',\omega) + \boldsymbol{G}_\mathrm{S}(\mathbf{r},\mathbf{r}',\omega), \tag{10.30}$$

where $\boldsymbol{G}_\mathrm{S}(\mathbf{r},\mathbf{r}',\omega)$ is the more or less complicated scattering part, which typically describes the effect of reflection at the (surfaces of discontinuity of the) bodies. Combining Eq. (10.27) with Eqs (10.29) and (10.30), we can write the

4) Γ corresponds to $\Gamma^{(\mathrm{r})}$ in Eq. (5.166) and the equations following. For notational convenience we drop the superscript here.

decay rate as[5]

$$\Gamma = \Gamma_0 + \frac{2\tilde{\omega}_{21}^2}{\hbar\varepsilon_0 c^2}\,\mathbf{d}_{21}\mathrm{Im}\,\boldsymbol{G}_{\mathrm{S}}(\mathbf{r}_A,\mathbf{r}_A,\tilde{\omega}_{21})\mathbf{d}_{21}\,. \tag{10.31}$$

In contrast to the homogeneous and isotropic free space, the decay rate now becomes a function of the atomic position and the orientation of the transition dipole moment. In other words, the homogeneous and isotropic vacuum fluctuations felt by an atom in the strictly free space are inhomogeneously and anisotropically changed by the presence of the bodies, in general. The nearer to a body that the atom is located, the stronger the effect to be expected.

Another effect of the bodies is that the spontaneous decay is not necessarily accompanied by the emission of a really observable photon, but instead a matter quantum can be created, because of material absorption (described in terms of the imaginary part of the permittivity). To quantify the effect, let us consider the emitted radiation energy W, which can be obtained by integration of $I(\mathbf{r},t)$ [Eq. (10.19)] with respect to time and integration over the surface of a sphere whose radius is much larger than the extension of the system under consideration,

$$W = 2c\epsilon_0 \lim_{\rho\to\infty}\int_0^\infty \mathrm{d}t \int_0^{2\pi}\mathrm{d}\phi\int_0^\pi \mathrm{d}\theta\,\rho^2\sin\theta\, I(\mathbf{r},t) \tag{10.32}$$

($\rho = |\mathbf{r}-\mathbf{r}_A|$). The ratio W/W_0 ($W_0 = \hbar\tilde{\omega}_{21}$), which is obviously a measure of the fraction of the emitted (radiation) energy, on average, can be regarded as the quantum yield on the time scale $\sim\Gamma^{-1}$. Accordingly, $1-W/W_0$ measures the fraction of the energy which is effectively absorbed by the bodies.

According to Eq. (10.19), together with Eqs (2.296) and (10.25), the intensity of the emitted radiation, $I(\mathbf{r},t)$, is given by

$$\begin{aligned} I(\mathbf{r},t) &= \left|\int_0^t \mathrm{d}t'\,\boldsymbol{K}_{(E)}^{(+)}(\mathbf{r},t;\mathbf{r}_A,t')\mathbf{d}_{12}e^{-(i\tilde{\omega}_{21}+\Gamma/2)t'}\right|^2 \\ &= \left|\frac{i}{\pi\varepsilon_0 c^2}\int_0^\infty \mathrm{d}\omega\,\frac{e^{-(i\tilde{\omega}_{21}+\Gamma/2)t}-e^{-i\omega t}}{i\omega-(i\tilde{\omega}_{21}+\Gamma/2)}\,\omega^2\mathrm{Im}\,\boldsymbol{G}(\mathbf{r},\mathbf{r}_A,\omega)\right|^2. \end{aligned} \tag{10.33}$$

In the free-space case, where $\boldsymbol{G}(\mathbf{r},\mathbf{r}',\omega)=\boldsymbol{G}_0(\mathbf{r},\mathbf{r}',\omega)$ is valid, with $\boldsymbol{G}_0(\mathbf{r},\mathbf{r}',\omega)$ being given by Eq. (2.298), straightforward calculation of the integral in Eq. (10.33) leads to

$$I_0(\mathbf{r},t) = \left(\frac{\tilde{\omega}_{21}^2 d_{21}\sin\theta}{4\pi\varepsilon_0 c^2\rho}\right)^2 e^{-\Gamma_0(t-\rho/c)}\Theta(t-\rho/c)+O(\rho^{-3}), \tag{10.34}$$

5) In fact, the imaginary part of the Green tensor at equal positions in Eq. (10.27) is singular for any realistic bulk material. Physically, this singularity is fictitious, because an atom, though surrounded by matter, should always be localized in a (more or less small) free-space region.

where the first term represents the relevant far-field intensity. It is straightforward to prove that Eq. (10.32) together with Eq. (10.34) leads to $W_0 = \hbar\tilde{\omega}_{21}$.

The effect of the body-induced change of the electromagnetic vacuum fluctuation can be used to control, to some extent, the process of spontaneous emission. So, spontaneous emission can be either enhanced [Purcell (1946)] or (almost) inhibited [Kleppner (1981)] compared with that in the free space. To be more specific, knowledge of the Green tensor for the body configuration of interest is required. It is worth noting that the Green tensor has been available for a large variety of configurations such as planar, spherically and cylindrically multi-layered ones [see, e. g., Tai (1994); Chew (1995)].

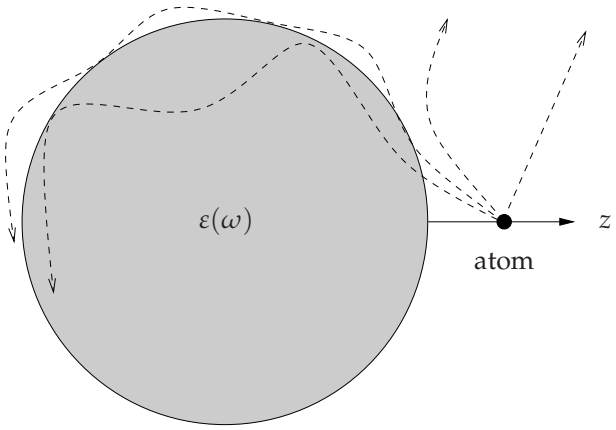

Fig. 10.1 Excited atom close to a dielectric microsphere. Possible ways of spontaneously emitting a photon are sketched by dashed arrows.

To give an impression of what can be observed, let us consider a two-level atom close to a dielectric microsphere (Fig. 10.1) whose permittivity is of the Drude–Lorentz type,

$$\epsilon(\omega) = 1 + \frac{\omega_{\mathrm{P}}^2}{\omega_{\mathrm{T}}^2 - \omega^2 - i\omega\gamma}\,. \tag{10.35}$$

Here ω_{P} corresponds to the coupling constant, and ω_{T} and γ are respectively the medium (transverse) oscillation frequency and the absorption linewidth. Note that the permittivity features a band gap between $\omega = \omega_{\mathrm{T}}$ and $\omega = \omega_{\mathrm{L}} = (\omega_{\mathrm{T}}^2 + \omega_{\mathrm{P}}^2)^{1/2}$. Figure 10.2 illustrates the dependence on the transition frequency of the decay rate. From the figure it is clearly seen that, when the atomic transition frequency agrees with (or is close to) the frequency of a field excitation of either whispering gallery type below the band gap ($\tilde{\omega}_{21} < \omega_{\mathrm{T}}$) or surface-guided type inside the band gap ($\omega_{\mathrm{T}} \leq \tilde{\omega}_{21} < \omega_{\mathrm{L}}$),[6] the spontaneous

6) The orthogonal modes obtained by solving the homogeneous Helmholtz equation for a dielectric sphere of constant and real permittivity are commonly called whispering gallery modes (surface-guided modes) in the case of positive (negative) permittivity.

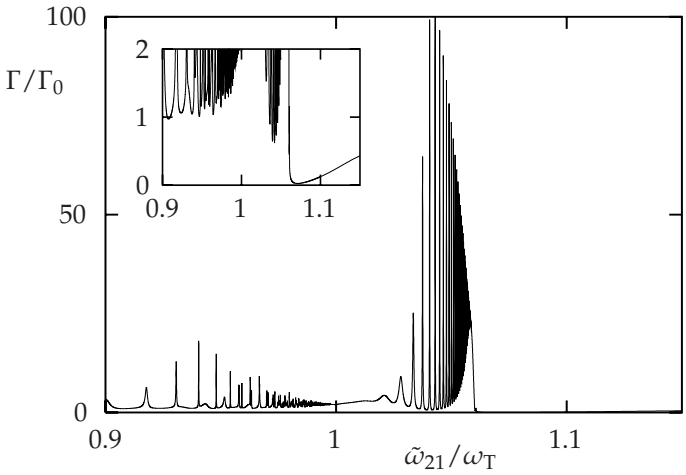

Fig. 10.2 The rate of spontaneous decay Γ of a two-level atom near a dielectric microsphere is shown as a function of the transition frequency $\tilde{\omega}_{21}$ for a radially oriented transition dipole moment, Γ_0 being the decay rate in free space [Eq. (10.29)]. The parameters in the permittivity (10.35) are chosen to be $\omega_P/\omega_T = 0.5$ and $\gamma/\omega_T = 10^{-4}$. The radius of the sphere is $R = 2\lambda_T$, and the distance between the atom and the surface of the sphere is $z_A = 0.1\,\lambda_T$ ($\lambda_T = 2\pi c/\omega_T$). [After Ho, Knöll and Welsch (2001).]

decay can be strongly enhanced. Figure 10.3 illustrates the fraction of the spontaneously emitted radiation energy, on average. The minima at the field resonance frequencies below the band gap indicate that, although the decay can be noticeably enhanced, the probability of emission of a really observable photon can be substantially reduced compared to the case of spontaneous emission in the free space. Obviously, a photon emitted at such a frequency is typically captured inside the microsphere for some time,[7] and hence the probability of photon absorption is increased. For transition frequencies inside the band gap, two regions can be distinguished. In the low-frequency region, where surface-guided waves are typically excited, radiative decay dominates, i. e., the atomic transition is accompanied by the emission of a photon escaping from the system. Here, the radiation penetration depth into the sphere is small and the probability of a photon being absorbed is also small. With increasing atomic transition frequency the penetration depth increases and the chance of a photon to escape drastically diminishes. As a result, photon absorption dominates.

7) This time, which is inversely proportional to the width of the respective field resonance line, is of course small compared with the decay time Γ^{-1}. Otherwise the Markov approximation fails (see Section 10.1.2).

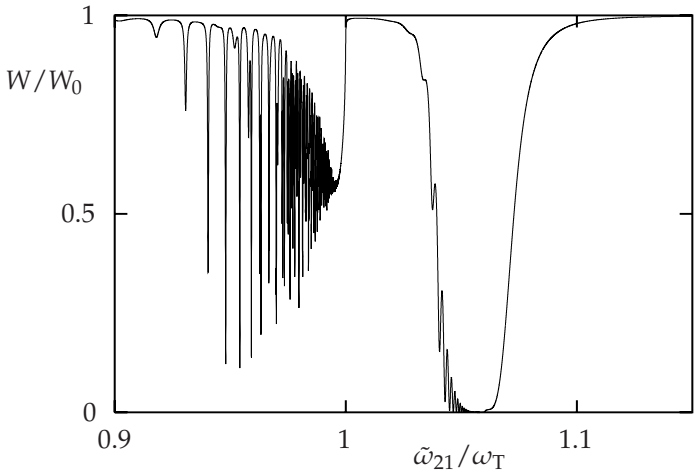

Fig. 10.3 The fraction W/W_0 of spontaneously emitted radiation of a two-level atom near a dielectric microsphere is shown as a function of the transition frequency $\tilde{\omega}_{21}$ for a radially oriented transition dipole moment. The other parameters are the same as in Fig. 10.2. [After Ho, Knöll and Welsch (2001).]

In particular, when the distance z_A between the atom and the surface of the sphere tends to zero,[8] then the decay rates $\Gamma^{\perp}$ and $\Gamma^{\parallel}$, respectively, for radially and tangentially oriented transition dipole moments approach the asymptotic values [Ho, Knöll and Welsch (2001)]

$$\Gamma^{\perp} = \frac{3\Gamma_0 c^3}{4\tilde{\omega}_{21}^3} \frac{\mathrm{Im}\,\varepsilon(\tilde{\omega}_{21})}{|\varepsilon(\tilde{\omega}_{21})+1|^2} \frac{1}{z_A^3}, \qquad \Gamma^{\parallel} = \tfrac{1}{2}\Gamma^{\perp}, \tag{10.36}$$

which solely result from absorption, as it is proportional to $\mathrm{Im}\,\varepsilon(\tilde{\omega}_{21})$. In other words, an effectively nonradiative decay is observed. The result reveals that, in the case of strong material absorption, the decay rate rises drastically as the atom approaches the surface of the microsphere, because of near-field assisted energy transfer from the atom to the medium – an effect that is typically observed for metals [see, e. g., Drexhage (1974)]. It should be pointed out that Eq. (10.36) also applies to the case of the atom being in front of a semi-infinite half space [Yeung and Gustafson (1996)], because in the short-distance limit the atom effectively regards the surface of the sphere as a plane.

10.1.1.2 **Level shift**

Let us return to the shift of the atomic transition frequency $\delta\omega_{21}$, Eq. (10.28). It reflects the fact that even in the case of an atom in the otherwise empty space,

8) Recall that z must not be smaller than typical interatomic distances in the sphere. Otherwise a microscopic treatment is required.

the unperturbed atomic energy levels are not the observed ones, because the interaction of the atom with the always present electromagnetic vacuum gives rise to level shifts. The effect usually called the Lamb shift[9] was first demonstrated experimentally by Lamb and Retherford (1947) [for the first calculation of the Lamb shift, see Bethe (1947)].

Substituting the decomposition according to Eq. (10.30) for the Green tensor in Eq. (10.28), one can see that the term arising from the free-space Green tensor $\boldsymbol{G}_0(\mathbf{r}_A, \mathbf{r}_A, \omega)$ is divergent and a refined description (including regularization) is required to adequately treat the ($\mathbf{r}_A$-independent) level shift caused by the interaction of the atom with the electromagnetic vacuum in free space.[10] To study the body-induced ($\mathbf{r}_A$-dependent) level shift, the shift observed in the free space may be thought of as being already included in the atomic transition frequency ω_{21}, so that ω_{21} is not the bare transition frequency but the transition frequency that is really observed in the free space, and thus $\delta\omega_{21}$ can be regarded as being determined by the scattering part of the Green tensor $\boldsymbol{G}_\mathrm{S}(\mathbf{r}_A, \mathbf{r}_A, \omega)$, leading to

$$\delta\omega_{21} = \frac{\mathcal{P}}{\pi\hbar\varepsilon_0 c^2} \int_0^\infty \mathrm{d}\omega\, \omega^2\, \frac{\mathbf{d}_{21}\mathrm{Im}\, \boldsymbol{G}_\mathrm{S}(\mathbf{r}_A, \mathbf{r}_A, \omega)\mathbf{d}_{12}}{\tilde{\omega}_{21} - \omega}\,. \tag{10.37}$$

The integral in Eq. (10.37) can be further evaluated by means of contour integral techniques to obtain

$$\delta\omega_{21} = \delta\omega_{21}^{(1)} + \delta\omega_{21}^{(2)}, \tag{10.38}$$

where

$$\delta\omega_{21}^{(1)} = -\frac{\tilde{\omega}_{21}^2}{\hbar\varepsilon_0 c^2}\, \mathbf{d}_{21}\mathrm{Re}\, \boldsymbol{G}_\mathrm{S}\,(\mathbf{r}_A, \mathbf{r}_A, \tilde{\omega}_{21})\mathbf{d}_{12} \tag{10.39}$$

and

$$\delta\omega_{21}^{(2)} = -\frac{\tilde{\omega}_{21}}{\pi\hbar\varepsilon_0 c^2} \int_0^\infty \mathrm{d}u\, u^2\, \frac{\mathbf{d}_{21}\boldsymbol{G}_\mathrm{S}(\mathbf{r}_A, \mathbf{r}_A, iu)\mathbf{d}_{12}}{\tilde{\omega}_{21}^2 + u^2}\,. \tag{10.40}$$

In fact, the off-resonant contribution $\delta\omega_{21}^{(2)}$ to the shift of the transition frequency is not complete, because – apart from the two-state model – the underlying rotating-wave approximation does not take into account the purely off-resonant lower-state level shift [cf. Section 10.2, Eqs (10.70)–(10.72)]. However, even if $\delta\omega_{21}^{(2)}$ is complemented by the missing terms, it would typically remain

9) More generally, the effect of level shifting observed when a dynamical system interacts with a dissipative system (Chapter 5) is also called Lamb shift.

10) For the problem of the level shift in free space, which has widely been studied, we refer the reader to the literature [e. g., Milonni (1994)].

small compared with the resonant contribution $\delta\omega_{21}^{(1)}$ and may be therefore disregarded in many cases. In this approximation, Eq. (10.38) reduces to

$$\delta\omega_{21} = -\frac{\tilde{\omega}_{21}^2}{\hbar\varepsilon_0 c^2}\,\mathbf{d}_{21}\mathrm{Re}\,\boldsymbol{G}_{\mathrm{S}}\,(\mathbf{r}_A,\mathbf{r}_A,\tilde{\omega}_{21})\mathbf{d}_{12}\,. \tag{10.41}$$

Whereas the effect of the bodies on the decay rate is determined by the imaginary part of the scattering part of the Green tensor, the real part is responsible for the shift of the transition frequency, as a comparison of Eq. (10.31) with Eq. (10.41) shows.

As in the case of the decay rate, further evaluation of Eq. (10.41) requires knowledge of the Green tensor for the actual body configuration. Again, the dependence of $\delta\omega_{21}$ on the distance z_A between an atom and the surface of a body in front of which the atom is situated becomes independent of the actual form of the body, if z_A is sufficiently small, leading to the short-distance law

$$\delta\omega_{21}^{\perp} = -\frac{3\Gamma_0 c^3}{16\tilde{\omega}_{21}^3}\,\frac{|\varepsilon(\tilde{\omega}_{21})|^2-1}{|\varepsilon(\tilde{\omega}_{21})+1|^2}\,\frac{1}{z_A^3}\,,\qquad \delta\omega_{21}^{\parallel} = \tfrac{1}{2}\delta\omega_{21}^{\perp} \tag{10.42}$$

[see, e. g., Ho, Knöll and Welsch (2001)]. This effect can be employed in scanning near-field optical microscopy to detect surface corrugation or impurities via the changes in the line shift of the radiation emitted by a probe atom, unless material absorption dominates the transition [see, e. g., Henkel and Sandoghdar (1998)]. The high sensitivity of the method results from the cubic dependence of the line shift on the inverse distance of the probe atom from the surface. As we will see in Section 10.2.1, body-induced level shifts are not only of spectroscopic relevance, but they are also closely related to the van der Waals force acting on an atom located near to macroscopic bodies.

10.1.2
Strong atom–field coupling

When a resonator-like arrangement of one or more macroscopic bodies features sharply peaked electromagnetic field resonances (such as the surface-guided waves or the whispering gallery waves in the case of a microsphere considered in Section 10.1.1, or the intra-cavity waves considered in Chapter 9) and the atomic transition frequency approaches the (mid-)frequency of such a resonator-assisted resonance line, then the strength of the atom–field coupling can drastically increase. More precisely, the correlation time, which in this case is determined by the inverse width of the resonator-assisted resonance line, can become much longer than the characteristic time scale on which the atomic-state population noticeably changes. As a consequence, the Markov approximation can fail and the temporal evolution of the occupation probability $|C_2(t)|^2$ of the upper atomic state can become nonexponential.

In order to gain insight into such a non-Markovian regime typical of strong atom–field coupling, let us consider a resonator-like equipment, referred to as cavity in the following, and assume that only one line of the cavity field, say the νth of (mid-)frequency ω_ν, is involved in the strong atom–field coupling – a case which requires the lines to be sufficiently well separated from each other in the relevant frequency interval. Accordingly we may decompose the integral kernel $\tilde{K}(t)$ as given by Eq. (10.23) together with Eq. (10.13) into two parts,

$$\tilde{K}(t) = \tilde{K}^{(1)}(t) + \tilde{K}^{(2)}(t), \tag{10.43}$$

where

$$\tilde{K}^{(1)}(t) = -\frac{1}{\hbar\pi\varepsilon_0 c^2}\int_{\omega_\nu-\frac{1}{2}\Delta\omega}^{\omega_\nu+\frac{1}{2}\Delta\omega} \mathrm{d}\omega\, \omega^2 e^{-i(\omega-\tilde{\omega}_{21})t}\mathbf{d}_{21}\mathrm{Im}\, \boldsymbol{G}(\mathbf{r}_A,\mathbf{r}_A,\omega)\mathbf{d}_{12}\,, \tag{10.44}$$

$\Delta\omega$ being a measure of the separation of two adjacent lines, is related to the cavity-resonance line under consideration, and $\tilde{K}^{(2)}(t)$ which is related to the residual cavity field may be regarded as being responsible for the shift of the atomic transition frequency, similar to Eq. (10.28). To further evaluate $\tilde{K}^{(1)}(t)$, let us assume that the cavity-resonance line can be approximated by a Lorentzian,

$$\tilde{K}^{(1)}(t) = -\frac{\omega_\nu^2 e^{i\delta_\nu t}}{\hbar\pi\varepsilon_0 c^2}\,\mathbf{d}_{21}\mathrm{Im}\, \boldsymbol{G}(\mathbf{r}_A,\mathbf{r}_A,\omega_\nu)\mathbf{d}_{12}\gamma_\nu^2\int_{\omega_\nu-\frac{1}{2}\Delta\omega}^{\omega_\nu+\frac{1}{2}\Delta\omega}\mathrm{d}\omega\,\frac{e^{-i(\omega-\omega_\nu)t}}{(\omega-\omega_\nu)^2+\gamma_\nu^2}\,, \tag{10.45}$$

where

$$\delta_\nu = \tilde{\omega}_{21} - \omega_\nu\,. \tag{10.46}$$

If the linewidth is sufficiently small compared with the line separation, i. e., $\gamma_\nu \ll \Delta\omega$, the upper (lower) limit of the integral may be extended to infinity (minus infinity), leading to

$$\tilde{K}^{(1)}(t) = -\tfrac{1}{2}\Gamma_\nu\gamma_\nu e^{i\delta_\nu t}e^{-\gamma_\nu|t|}, \tag{10.47}$$

where Γ_ν is defined according to Eq. (10.27), with $\tilde{\omega}_{21}$ being replaced with ω_ν,

$$\Gamma_\nu = \frac{2\omega_\nu^2}{\hbar\varepsilon_0 c^2}\,\mathbf{d}_{21}\mathrm{Im}\, \boldsymbol{G}(\mathbf{r}_A,\mathbf{r}_A,\omega_\nu)\mathbf{d}_{12}. \tag{10.48}$$

Hence the integro-differential equation (10.22) approximates to

$$\begin{aligned}\dot{\tilde{C}}_2(t) &= \int_0^t \mathrm{d}t'\,\tilde{K}^{(1)}(t-t')\tilde{C}_2(t') \\ &= -\tfrac{1}{2}\Gamma_\nu\gamma_\nu\int_0^t \mathrm{d}t'\, e^{(i\delta_\nu-\gamma_\nu)(t-t')}\tilde{C}_2(t'),\end{aligned} \tag{10.49}$$

which corresponds to the differential equation

$$\ddot{\tilde{C}}_2(t) - (i\delta_\nu - \gamma_\nu)\dot{\tilde{C}}_2(t) + \tfrac{1}{4}\Omega_\nu^2 \tilde{C}_2(t) = 0 \tag{10.50}$$

$[\tilde{C}_2(0)=1, \dot{\tilde{C}}_2(0)=0]$, where

$$\Omega_\nu = \sqrt{2\Gamma_\nu \gamma_\nu} \tag{10.51}$$

is the vacuum Rabi frequency with respect to the νth resonance line of the cavity field.

Equation (10.50) can be solved by means of the standard ansatz $\tilde{C}_2(t) \sim e^{\lambda t}$, leading to

$$\lambda^2 - (i\delta_\nu - \gamma_\nu)\lambda + \tfrac{1}{4}\Omega_\nu^2 = 0, \tag{10.52}$$

from which

$$\lambda = \tfrac{1}{2}(i\delta_\nu - \gamma_\nu) \pm \tfrac{1}{2}\sqrt{(i\delta_\nu - \gamma_\nu)^2 - \Omega_\nu^2} \tag{10.53}$$

follows. Strong atom–field coupling requires that the inequalities[11]

$$|\delta_\nu| \ll \Omega_\nu, \quad \gamma_\nu \ll \Omega_\nu \tag{10.54}$$

are fulfilled. Hence the square root on the right-hand side of Eq. (10.53) may be expanded to linear order in δ_ν and γ_ν to approximately obtain

$$\lambda = \tfrac{1}{2}(\pm\Omega_\nu + \delta_\nu)i - \tfrac{1}{2}\gamma_\nu\,, \tag{10.55}$$

leading to

$$\begin{aligned}\tilde{C}_2(t) &= e^{\frac{1}{2}(i\delta_\nu - \gamma_\nu)t}\Big[\cos\big(\tfrac{1}{2}\Omega_\nu t\big) - \frac{i\delta_\nu - \gamma_\nu}{\Omega_\nu}\,\sin\big(\tfrac{1}{2}\Omega_\nu t\big)\Big] \\ &\simeq e^{\frac{1}{2}(i\delta_\nu - \gamma_\nu)t}\cos\big(\tfrac{1}{2}\Omega_\nu t\big).\end{aligned} \tag{10.56}$$

In contrast to the irreversible exponential decay of the upper-state occupation probability which is typical of weak atom–field coupling, damped (vacuum) Rabi oscillations are typically observed in the case of strong atom–field coupling. In particular, on the time scale $\sim \Omega_\nu^{-1}$ the atom and the cavity field periodically exchange excitation – a process which is not disturbed by dissipation so that it becomes reversible on this time scale:

$$\begin{aligned}|\tilde{C}_2(t)|^2 = |C_2(t)|^2 &= 1 - |C_1(t)|^2 = \cos^2\big(\tfrac{1}{2}\Omega_\nu t\big) \\ &= \tfrac{1}{2}[1 + \cos(\Omega_\nu t)].\end{aligned} \tag{10.57}$$

11) Note that the second condition implies a sufficiently high-Q cavity with respect of the νth line, in general ($Q = \omega_\nu/\gamma_\nu \gg 1$).

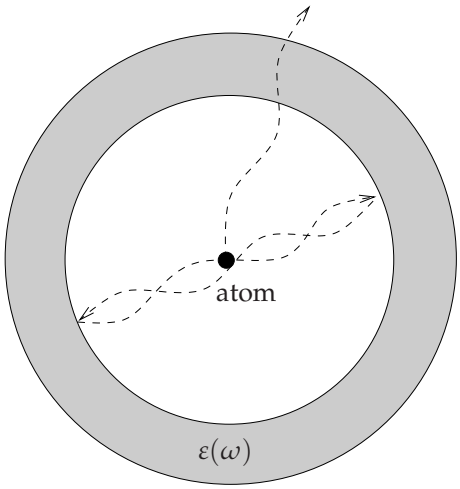

Fig. 10.4 Atom at the center of a dielectric spherical-shell cavity. Possible waves which an excited atom can spontaneously emit are sketched by dashed arrows.

Physically this means that a photon spontaneously emitted by the atom in the upper quantum state will be reabsorbed by the atom in the further course of time, thereby again exciting the atom, and the cycle of photon emission and reabsorption begins anew. The process can be obviously described by resonantly coupling the two-level atom to a single mode of an ideal cavity ($Q \to \infty$). Though only valid on a time scale that is sufficiently short compared with the inverse of the small, but always finite, width of the cavity line with which the atom strongly interacts, one advantage of such a model of strong atom–field coupling – known as the Jaynes–Cummings model (Section 12.1) – is the fact that the effect of arbitrarily excited states of the cavity field can be included in the theory more easily than would be the case in the exact description.

To illustrate the effect of strong atom–field coupling, let us consider an excited two-level atom located at the center of a dielectric spherical-shell cavity (Fig. 10.4). Typical examples of the temporal evolution of the occupation probability $|C_2(t)|^2$ of the upper atomic state are shown in Fig. 10.5. They were obtained by numerical integration of the exact integral equation (10.14), with the permittivity being of Drude–Lorentz type according to Eq. (10.35), by assuming the atomic transition being tuned to a cavity-resonance line in the middle of the band gap. The figure reveals that, with decreasing value of γ_ν (increasing Q value), the Rabi oscillations become more and more pronounced, in full agreement with Eq. (10.56).

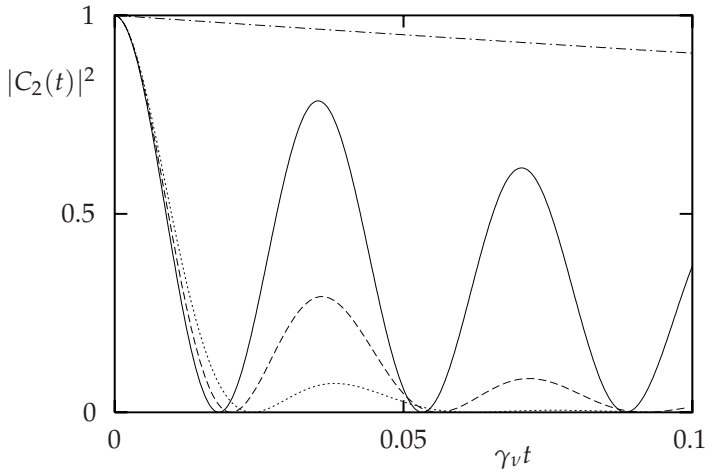

Fig. 10.5 The temporal evaluation of the occupation probability $|C_2(t)|^2$ of the upper atomic state is shown for an atom at the center of a spherical-shell cavity of inner radius $R = 30\,\lambda_T$ and thickness $d = \lambda_T$ [$\omega_P/\omega_T = 0.5$, $\tilde{\omega}_{21}/\omega_T$ $\tilde{\omega}_\nu/\omega_T = 1.046448$, $\Gamma_0\lambda_T/(2c) = 10^{-6}$; $\gamma_\nu/\omega_T = 10^{-4}$ (solid line), $\gamma_\nu/\omega_T = 5 \times 10^{-4}$ (dashed line), $\gamma_\nu/\omega_T = 10^{-3}$ (dotted line). For comparison, the exponential decay in free space (dash-dotted line) is shown. [After Ho, Knöll and Welsch (2000).]

10.2 Vacuum forces

It is well known that there is an attractive force between electrically neutral, unpolarized ground-state atoms or molecules. This force, also called the van der Waals force, represents a pure quantum effect. Restricting his attention to two-level atoms and employing fourth-order time-independent perturbation theory, London (1930) derived the potential associated with the force to be

$$U(r) = -\frac{3\hbar\omega_{21}\alpha_{\mathrm{stat}}^2}{4r^6} \tag{10.58}$$

(r, distance between the atoms; α_{stat}, static atomic polarizability). Verwey and Overbeek (1948) had already pointed out that the r^{-6} potential does not apply in the retarded limit, i. e., when the separation of the atoms is large compared with the atomic transition wavelength. A consistent quantum mechanical theory which closed this loophole was then given by Casimir and Polder (1948).[12] In particular, they found that, for large interatomic separations, the van der Waals potential varies as r^{-7} due to retardation. Moreover, the theory clearly showed that the origin of the force must be seen in the interaction of the atoms with the fluctuating electromagnetic quantum vacuum.

12) In this context, van der Waals forces are also referred to as Casimir–Polder forces.

Forces of van der Waals type are not only observed on a microscopic level but also on a macroscopic level. Typical examples are the force (also referred to as the van der Waals force) to which an atom is subject in the presence of macroscopic bodies, or the force (referred to as the Casimir force) between macroscopic bodies – dense media that may be thought of as consisting of a huge number of interacting atoms. Both types of force can be regarded as being macroscopic manifestations of microscopic van der Waals forces. In the following we restrict our attention to dielectric bodies, noting that the theory can also be extended to other materials.

10.2.1 Force on an atom

From Eq. (2.10) we know that the classical Lorentz force density $\mathbf{f}_{\mathrm{L}}(\mathbf{r})$ acting on a charge density $\rho(\mathbf{r})$ and a current density $\mathbf{j}(\mathbf{r})$ in an electric field $\mathbf{E}(\mathbf{r})$ and an induction field $\mathbf{B}(\mathbf{r})$ reads

$$\mathbf{f}_{\mathrm{L}}(\mathbf{r}) = \rho(\mathbf{r})\mathbf{E}(\mathbf{r}) + \mathbf{j}(\mathbf{r}) \times \mathbf{B}(\mathbf{r}), \tag{10.59}$$

and the total Lorentz force acting on the matter contained inside some space region (of volume V) can be obtained according to

$$\mathbf{F} = \int_V \mathrm{d}^3 r\, \mathbf{f}_{\mathrm{L}}(\mathbf{r}). \tag{10.60}$$

In the case of neutral matter which is electrically polarizable, the charge and current densities can be regarded as being the polarization charge and current densities $\rho_{\mathrm{P}}(\mathbf{r})$ and $\mathbf{j}_{\mathrm{P}}(\mathbf{r})$, respectively, so that in Eq. (10.59) we may set

$$\rho(\mathbf{r}) = \rho_{\mathrm{P}}(\mathbf{r}) = -\boldsymbol{\nabla}\mathbf{P}(\mathbf{r}) \tag{10.61}$$

and

$$\mathbf{j}(\mathbf{r}) = \mathbf{j}_{\mathrm{P}}(\mathbf{r}) = \dot{\mathbf{P}}(\mathbf{r}). \tag{10.62}$$

Let us consider a neutral, electrically polarizable atom at position $\mathbf{r}_A$ and restrict our attention to the electric-dipole approximation, i. e.,

$$\mathbf{P}(\mathbf{r}) \equiv \mathbf{P}_A(\mathbf{r}) = \mathbf{d}\delta(\mathbf{r} - \mathbf{r}_A). \tag{10.63}$$

Combining Eqs (10.59)–(10.63), we find that the Lorentz force acting on the atom can be given in the form

$$\begin{aligned}\mathbf{F} &= \mathbf{d}\boldsymbol{\nabla}_A \otimes \mathbf{E}(\mathbf{r}_A) + \dot{\mathbf{d}} \times \mathbf{B}(\mathbf{r}_A) \\ &= \boldsymbol{\nabla} \otimes \mathbf{d}\mathbf{E}(\mathbf{r})\big|_{\mathbf{r}=\mathbf{r}_A} + \left.\frac{\partial[\mathbf{d} \times \mathbf{B}(\mathbf{r})]}{\partial t}\right|_{\mathbf{r}=\mathbf{r}_A}\end{aligned} \tag{10.64}$$

($\boldsymbol{\nabla}_A \mathrel{\widehat{=}} \partial/\partial x_{Ak}$), where the second line follows from the first one by using the Maxwell equation (2.2). Equation (10.64), which as an operator-valued equation is also valid in quantum theory, may serve as a starting point for calculating the radiation force acting (in the electric-dipole approximation) on a neutral atom, by taking the expectation value with respect to the internal atomic quantum state (i. e., the electronic quantum state in the case of an atom) and the quantum state of the electromagnetic field,

$$\mathbf{F} = \boldsymbol{\nabla} \langle \hat{\mathbf{d}} \hat{\mathbf{E}}(\mathbf{r}) \rangle \big|_{\mathbf{r}=\mathbf{r}_A} + \frac{\partial \langle \hat{\mathbf{d}} \times \hat{\mathbf{B}}(\mathbf{r}) \rangle}{\partial t} \bigg|_{\mathbf{r}=\mathbf{r}_A} . \tag{10.65}$$

This equation can be interpreted in several ways. So it can be regarded as giving the force in the Newtonian equation of motion for the center-of-mass coordinate, which is further evaluated within the frame of quantum mechanics or, if possible, also within the frame of classical mechanics. Clearly, the center-of-mass motion should be sufficiently slow, so that it (approximately) decouples from the internal motion in the spirit of a Born-Oppenheimer approximation. Equation (10.65) can be also regarded as determining the force that must be compensated for in the case when the center-of-mass coordinate may be considered as a given (classical) parameter controlled externally. Since there is no need here to distinguish between the possible interpretations, we do not use the operator hat on the center-of-mass coordinate $\mathbf{r}_A$ in Eq. (10.65). In particular, when the atom–field system is prepared in an energy eigenstate, then the expectation value of the magnetic part of the force obviously vanishes, so that only the expectation value of the electric part needs to be considered, i. e.,

$$\mathbf{F} = \boldsymbol{\nabla} \langle \hat{\mathbf{d}} \hat{\mathbf{E}}(\mathbf{r}) \rangle \big|_{\mathbf{r}=\mathbf{r}_A} . \tag{10.66}$$

To calculate the van der Waals force which is observed in the case when the atom is subject to a body-assisted electromagnetic vacuum, we restrict our attention to energy eigenstates. In this case Eq. (10.66) applies, and a comparison with the (multipolar-coupling) interaction energy (2.239)[13] may suggest, at first glance, that the interaction energy plays the role of the potential of the force. However, the exact state vector with which the expectation value is calculated introduces an additional $\mathbf{r}_A$ dependence, which prevents this idea from being true in general. Fortunately, the expectation value calculated with the state vector in the lowest (leading) order of perturbation theory is an exception, so that in this most commonly considered case, the force can be simply obtained by taking the negative gradient of the (position-dependent) part

13) Note that Eq. (10.64) also holds with $\mathbf{E}$ being replaced by the transformed $\mathbf{E}'$, so that in the further calculations the prime can be omitted for notational convenience.

of the body-induced shift of the corresponding energy, as we will do in the following.

10.2.1.1 Lowest-order perturbation theory

Let the body-assisted electromagnetic field be in the ground state and the atom in the nth energy eigenstate. The interaction Hamiltonian (2.239) in the form of Eq. (2.243) implies that the lowest-order energy shift δE_n is obtained in the second order of the perturbation series of the energy, i. e.,

$$\delta E_n = -\frac{1}{\hbar}\sum_k \mathcal{P}\int_0^\infty \mathrm{d}\omega \int \mathrm{d}^3 r\, \frac{|\langle n|\langle\{0\}|\hat{H}_{\mathrm{int}}|\{\mathbf{1}(\mathbf{r},\omega)\}\rangle|k\rangle|^2}{\omega_{kn}+\omega} \tag{10.67}$$

[$\omega_{kn} = (E_k - E_n)/\hbar$ are the unperturbed transition frequencies], where [recall Eqs (10.7) and (10.8)]

$$\begin{aligned}\langle n|\langle\{0\}|\hat{H}_{\mathrm{int}}|\{\mathbf{1}(\mathbf{r},\omega)\}\rangle|k\rangle &= -\langle n|\langle\{0\}|\hat{\mathbf{d}}\hat{\mathbf{E}}(\mathbf{r}_A)|\{\mathbf{1}(\mathbf{r},\omega)\}\rangle|k\rangle \\ &= -i\sqrt{\frac{\hbar}{\pi\varepsilon_0}}\,\frac{\omega^2}{c^2}\,\sqrt{\mathrm{Im}\,\varepsilon(\mathbf{r},\omega)}\,\mathbf{d}_{nk}\boldsymbol{G}(\mathbf{r}_A,\mathbf{r},\omega).\end{aligned} \tag{10.68}$$

Combining Eqs (10.67) and (10.68) yields

$$\begin{aligned}\delta E_n = -\frac{1}{\pi\varepsilon_0 c^4}\sum_k \mathcal{P}\int_0^\infty \mathrm{d}\omega \Bigg[&\frac{\omega^4}{\omega_{kn}+\omega} \\ &\times \int \mathrm{d}^3 r\, \mathrm{Im}\,\varepsilon(\mathbf{r},\omega)\mathbf{d}_{nk}\boldsymbol{G}(\mathbf{r}_A,\mathbf{r},\omega)\boldsymbol{G}^*(\mathbf{r},\mathbf{r}_A,\omega)\mathbf{d}_{kn}\Bigg],\end{aligned} \tag{10.69}$$

which, with the help of the relation (A.3), can be performed to obtain

$$\delta E_n = -\frac{1}{\pi\varepsilon_0 c^2}\sum_k \mathcal{P}\int_0^\infty \mathrm{d}\omega\, \frac{\omega^2 \mathbf{d}_{nk}\mathrm{Im}\,\boldsymbol{G}(\mathbf{r}_A,\mathbf{r}_A,\omega)\mathbf{d}_{kn}}{\omega_{kn}+\omega}\,. \tag{10.70}$$

Before proceeding let us briefly make contact with the frequency shift $\delta\omega_{21}$ as given by Eq. (10.28). We first note that from Eq. (10.70) the shifted transition frequencies $\tilde{\omega}_{nm}$ can be calculated according to

$$\tilde{\omega}_{nm} = \hbar^{-1}[E_n + \delta E_n - (E_m + \delta E_m)] = \omega_{nm} + \delta\omega_{nm}, \tag{10.71}$$

where the frequency shifts are given by

$$\delta\omega_{nm} = \hbar^{-1}(\delta E_n - \delta E_m). \tag{10.72}$$

Comparing $\delta\omega_{21}$ calculated from Eq. (10.72) [together with Eq. (10.70)] with $\delta\omega_{21}$ from Eq. (10.28), we see, on identifying $\tilde{\omega}_{21}$ in Eq. (10.28) with the unperturbed transition frequency ω_{21}, that in the rotating-wave approximation

used to derive Eq. (10.28), the off-resonant lower-state level shift is completely ignored. Further, in Eq. (10.28) only the term with $k=1$ in the sum for δE_2 in Eq. (10.70) is taken into account, which is of course a consequence of the two-level approximation.

As already mentioned in Section 10.1.1, the body-induced level shifts in which we are interested are determined by the scattering part of the Green tensor [recall the decomposition (10.30) of the Green tensor]. Hence the potential $U_n(\mathbf{r}_A)$ for the van der Waals force

$$\mathbf{F}_n(\mathbf{r}_A) = -\boldsymbol{\nabla}_A U_n(\mathbf{r}_A) \tag{10.73}$$

can be obtained from Eq. (10.70) by replacing therein the Green tensor by its scattering part:

$$U_n(\mathbf{r}_A) = -\frac{1}{\pi\varepsilon_0 c^2}\sum_k \mathcal{P}\int_0^\infty \mathrm{d}\omega\, \frac{\omega^2 \mathbf{d}_{nk}\mathrm{Im}\, \boldsymbol{G}_{\mathbf{S}}(\mathbf{r}_A,\mathbf{r}_A,\omega)\mathbf{d}_{kn}}{\omega_{kn}+\omega}\,. \tag{10.74}$$

Applying contour integral techniques, we may decompose the van der Waals potential $U_n(\mathbf{r}_A)$ into two parts [cf. Eqs (10.37)–(10.40)],

$$U_n(\mathbf{r}_A) = U_n^{(1)}(\mathbf{r}_A) + U_n^{(2)}(\mathbf{r}_A), \tag{10.75}$$

where

$$U_n^{(1)}(\mathbf{r}_A) = -\frac{1}{\varepsilon_0 c^2}\sum_k \Theta(\omega_{nk})\omega_{nk}^2 \mathbf{d}_{nk}\mathrm{Re}\, \boldsymbol{G}_{\mathrm{S}}(\mathbf{r}_A,\mathbf{r}_A,\omega_{nk})\mathbf{d}_{kn} \tag{10.76}$$

is the resonant part and

$$U_n^{(2)}(\mathbf{r}_A) = \frac{1}{\pi\varepsilon_0 c^2}\sum_k \int_0^\infty \mathrm{d}u\, u^2\, \frac{\omega_{kn}\mathbf{d}_{nk}\boldsymbol{G}_{\mathrm{S}}(\mathbf{r}_A,\mathbf{r}_A,iu)\mathbf{d}_{kn}}{\omega_{kn}^2+u^2} \tag{10.77}$$

the off-resonant part. In order to bring Eq. (10.77) into a more compact form, it may be convenient to introduce the lowest-order polarizability tensor[14] attributed to the atom in the nth excited state, viz.

$$\boldsymbol{\alpha}_n(\omega) \equiv \boldsymbol{\alpha}_n^{(0)}(\omega) = \lim_{\epsilon\to 0}\frac{2}{\hbar}\sum_k \frac{\omega_{kn}\mathbf{d}_{nk}\otimes\mathbf{d}_{kn}}{\omega_{kn}^2-\omega^2-i\omega\epsilon}\,, \tag{10.78}$$

leading to

$$U_n^{(2)}(\mathbf{r}_A) = \frac{\hbar}{2\pi\varepsilon_0 c^2}\int_0^\infty \mathrm{d}u\, u^2 \mathrm{Tr}\big[\boldsymbol{\alpha}_n(iu)\boldsymbol{G}^{(1)}(\mathbf{r}_A,\mathbf{r}_A,iu)\big]. \tag{10.79}$$

14) See, e. g., Fain and Khanin (1969).

In particular, for an atom in a spherically symmetric state, Eqs (10.76) and (10.79) simplify to

$$U_n^{(1)}(\mathbf{r}_A) = -\frac{1}{3\varepsilon_0 c^2}\sum_k \Theta(\omega_{nk})\omega_{nk}^2|\mathbf{d}_{nk}|^2 \mathrm{Tr}\,[\mathrm{Re}\,\boldsymbol{G}_\mathrm{S}(\mathbf{r}_A,\mathbf{r}_A,\omega_{nk})] \tag{10.80}$$

and

$$U_n^{(2)}(\mathbf{r}_A) = \frac{\hbar}{2\pi\varepsilon_0 c^2}\int_0^\infty \mathrm{d}u\, u^2 \alpha_n(iu)\,\mathrm{Tr}\,\boldsymbol{G}_\mathrm{S}(\mathbf{r}_A,\mathbf{r}_A,iu). \tag{10.81}$$

To obtain Eq. (10.81) from Eq. (10.79), we have used the relation $\boldsymbol{\alpha}_n(\omega) = \alpha_n(\omega)\boldsymbol{I}$, where

$$\alpha_n(\omega) = \lim_{\epsilon\to 0}\frac{2}{3\hbar}\sum_k \frac{\omega_{kn}|\mathbf{d}_{nk}|^2}{\omega_{kn}^2-\omega^2-i\omega\epsilon}\,. \tag{10.82}$$

Equation (10.75), together with Eqs (10.76) and (10.77) [or, equivalently, (10.79)], apply to arbitrary causal dielectric bodies which linearly and locally respond to the electric field;[15] all relevant information on the bodies is contained in the scattering Green tensor. From Eq. (10.76) it is seen that [because of $\Theta(\omega_{nk})$] $U_n^{(1)}(\mathbf{r}_A)$ can only contribute to $U_n(\mathbf{r}_A)$ if the atom is excited. In this case $U_n^{(1)}(\mathbf{r}_A)$ can be expected to be the dominant contribution in general. It should be pointed out that since an excited state decays in the further course of time, the force acting on an initially excited atom varies with time until the atom has arrived back at the ground state – an effect that requires a dynamic description rather than the static one considered here [for a dynamic description, see Buhmann, Knöll, Welsch and Ho (2004)]. Note that the dipole matrix elements which enter the spontaneous decay rate attributed to an excited state also enter the excited-state van der Waals potential.

Let us study the van der Waals potential $U(\mathbf{r}_A) \equiv U_0(\mathbf{r}_A) = U_0^{(2)}(\mathbf{r}_A)$ of a ground-state atom in more detail. According to Eq. (10.81) it reads

$$U(\mathbf{r}_A) = \frac{\hbar}{2\pi\varepsilon_0 c^2}\int_0^\infty \mathrm{d}u\, u^2 \alpha(iu)\,\mathrm{Tr}\,\boldsymbol{G}_\mathrm{S}(\mathbf{r}_A,\mathbf{r}_A,iu). \tag{10.83}$$

[$\alpha(\omega)\equiv\alpha_0(\omega)$]. From Eq. (10.83) it is clearly seen that the van der Waals force acting on a nonexcited, electrically neutral, polarizable particle, represents a quantum effect, which would vanish if $\hbar$ were set equal to zero in Eq. (10.83).[16] It is basically a pure vacuum effect, because the overall system is in the ground

15) It can be shown that Eq. (10.75) together with Eqs (10.76) and (10.77) [or, equivalently, (10.79)] also apply to causally, linearly and locally responding magnetodielectric bodies [Buhmann, Knöll, Welsch and Ho (2004)].

16) Note that the (scattering part of the) Green tensor is a classical quantity and the polarizability can also be introduced classically.

state, and hence a fully quantum theoretical treatment is necessary. By contrast, if the atom is in an excited state, the resonant contribution $U_n^{(1)}(\mathbf{r}_A)$ as given by Eq. (10.76) can be understood, in a sense, on the basis of a quasi-classical description, by considering the interaction of an oscillating classical dipole with the field scattered by the bodies.

10.2.1.2 Atom in front of a planar body

To give a typical example of the van der Waals potential of a ground-state atom, let us consider an atom in front of a planar body. It can be calculated in a straightforward way by inserting in Eq. (10.83) the well-known (scattering part of the) Green tensor for a multi-layer dielectric plate of infinite lateral extension.[16] Since the calculation is somewhat lengthy, we renounce it here and present the result at once:

$$U(z_A) = \frac{\hbar\mu_0}{8\pi^2}\int_0^\infty \mathrm{d}u\, u^2\alpha(iu)\int_0^\infty \mathrm{d}q\,\frac{q}{\kappa}\,e^{-2\kappa z_A}\left[r_{s-} - \left(1+2\frac{q^2c^2}{u^2}\right)r_{p-}\right]. \tag{10.84}$$

Here, the atom is on the right of the plate, with z_A being the (positive) distance between the surface of the plate and the atom (see Fig. 10.6). Further, q is the absolute value of the transverse (lateral) component $\mathbf{q}$ of the wave vector $\mathbf{k}$, and $r_{\sigma-}$ ($\sigma = s, p$) are the (generalized) reflection coefficients for s-polarized and p-polarized waves[17] with respect to the surface (at $z=0$) which faces the atom, and

$$\kappa = \kappa(iu, q) = \sqrt{q^2 - \frac{(iu)^2}{c^2}}\,. \tag{10.85}$$

Since, depending on the actual layer structure of the plate, the reflection coefficients $r_{\sigma-} = r_{\sigma-}(iu, q)$ can be more or less complicated functions of u and

16) For a suitable representation of the Green tensor for a multi-layer dielectric structure of infinite lateral extension, see, e. g., Tomaš (1995). Since the transverse projection $\mathbf{q}$ of the wave vector is conserved and the polarizations $\sigma = s, p$ decouple, the scattering part of the Green tensor within each layer can be expressed in terms of reflection coefficients $r_{\sigma\pm} = r_{\sigma\pm}(\omega, q)$ referring to reflection of waves at the right (+) and left (−) wall (formed by the respective layers), as seen from the layer under consideration. Explicit (recurrence) expressions for the reflection coefficients are available if the walls are multi-slab magnetodielectrics like Bragg mirrors. For continuous wall profiles, Riccati-type equations have to be solved [Chew (1995)].

17) The corresponding polarization vectors are $\mathbf{e}_{s-} = \mathbf{q}/q \times \mathbf{e}_z$ and $\mathbf{e}_{p-} = -(iq\mathbf{e}_z - \kappa\mathbf{q}/q)/k$.

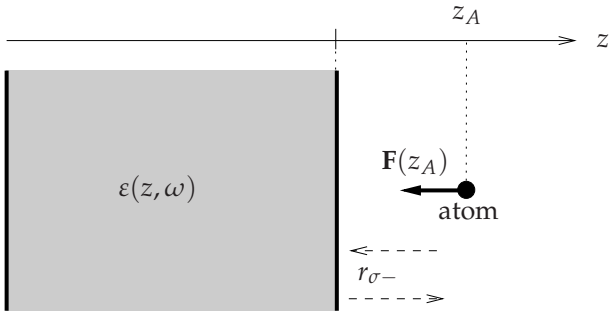

Fig. 10.6 A ground-state atom near to a (multi-layer) dielectric plate is subject to an attractive force $\mathbf{F}(z_A)$, Eq. (10.84), which, for chosen atomic position z_A, is determined by the (zeroth-order) atomic polarizability and the (generalized) reflection coefficients $r_{\sigma-}$ ($\sigma = s, p$). Note that only virtual photons are involved in the scattering at the plate.

q, further evaluation of the integrals in Eq. (10.84) requires application of numerical methods, in general.

In the limiting case of a perfectly reflecting plate such that

$$r_{p-} = -r_{s-} = 1, \tag{10.86}$$

the second integral in Eq. (10.84) can be easily calculated, leading to the attractive potential

$$U(z_A) = -\frac{\hbar}{16\pi^2\varepsilon_0 z_A^3}\int_0^\infty \mathrm{d}u\,\alpha(iu)e^{-2uz_A/c}\left[1+2\left(\frac{uz_A}{c}\right)+2\left(\frac{uz_A}{c}\right)^2\right], \tag{10.87}$$

which is exactly the formula first derived by Casimir and Polder (1948) for the potential of a ground-state atom in front of a perfectly conducting plate. In the short-distance (i. e., nonretarded) limit we may approximately set $e^{-2uz_A/c} = 1$ in the integral in Eq. (10.87) and neglect the second and third terms in the square brackets to recover, on using Eq. (10.82), the result of Lennard-Jones (1932):

$$U(z_A) = -\frac{1}{48\pi\varepsilon_0}\frac{1}{z_A^3}\sum_k |\mathbf{d}_{0k}|^2 = -\frac{\langle 0|\hat{\mathbf{d}}^2|0\rangle}{48\pi\varepsilon_0}\frac{1}{z_A^3}. \tag{10.88}$$

In the long-distance (i. e., retarded) limit the atomic polarizability $\alpha(iu)$ may be approximately replaced by its static value $\alpha(0)$ and put in front of the integral, leading to

$$U(z_A) = -\frac{3\hbar c\alpha(0)}{32\pi^2\varepsilon_0}\frac{1}{z_A^4}. \tag{10.89}$$

As already mentioned, the general formulas that do not explicitly make use of the material properties are also valid for other materials than dielectrics. Hence relations other than the ones given in Eq. (10.86) might be attributed to a perfectly reflecting plate. In particular, when $r_{p-} = -r_{s-} = -1$ is set, then the expression in the square brackets in Eq. (10.84) changes the sign; hence $U(z_A)$ changes to $-U(z_A)$ and as a result a repulsive force is observed. This case of a perfectly reflecting plate would correspond to an infinitely permeable magnetic plate – a case which is, of course, far from reality. Nevertheless, it reveals a very general aspect. The fact that Maxwell's equations in the absence of (free) charges and currents are invariant under a duality transformation between electric and magnetic fields can be exploited to extend the notion of forces acting on electrically polarizable objects to magnetically polarizable objects. Thus, knowing the attractive van der Waals force between two electrically polarizable particles (e. g., atoms), one can infer the existence of an analogous attractive force between two magnetically polarizable particles, which may be obtained from the former by replacing the electric polarizabilities by the corresponding magnetic ones. In contrast, the force between two polarizable particles of opposite type is repulsive [Feinberg and Sucher (1970)], which implies that an atom in front of a magnetic plate is subject to a repulsive force.

The van der Waals potential $U_n(\mathbf{r}_A)$ as given by Eq. (10.75) together with Eqs (10.76) and (10.77) [or (10.79)] is the body-induced shift of the (unperturbed) atomic energy level E_n. This offers the possibility of measuring it by means of spectroscopic methods. In particular, the powerful methods of laser spectroscopy used in cavity QED to study fundamental quantum phenomena can be employed also to perform direct and precise measurements of the van der Waals coupling between an atom and cavity walls, in which the interaction is quantitatively studied as a function of controlled separation and of the electronic state of the atom [Sandoghdar, Sukenik, Hinds and Haroche (1992)].

10.2.2 The Casimir force

In classical electrodynamics, electrically neutral material bodies at zero temperature which do not carry a permanent polarization (and/or magnetization) are not subject to a Lorentz force in the absence of external electromagnetic fields. The situation changes in quantum electrodynamics, since the body-assisted vacuum fluctuations of the electromagnetic field can give rise to a nonvanishing Lorentz force – the Casimir force. Let us assume that the macroscopic bodies consist of distinguishable, polarizable microconstituents commonly called atoms or molecules within the framework of molecular optics. From Section 10.2.1 it is clear that in the case of a large collection of (ground-state) atoms forming a macroscopic body, a van der Waals interaction of the

body with other bodies should be observed. Clearly, the resulting Casimir force between macroscopic bodies is in general not simply the sum of the van der Waals forces acting on single (ground-state) atoms, because of many-particle interactions [see, e .g, Buhmann and Welsch (2006)]. Fortunately, the interaction of electromagnetic fields with linear magnetodielectric matter can be expressed, via the permittivity and the permeability, in terms of the Green tensor which a priori takes into account many-particle interactions. Hence, the Casimir force expressed in terms of the Green tensor takes into account many-particle interactions as well.

10.2.2.1 Basic equations

Let us again restrict our attention to dielectric bodies[19] and begin with the classical Lorentz force as given by Eq. (10.60) together with Eqs (10.59), (10.61) and (10.62). In contrast to Eq. (10.63), $\mathbf{P}(\mathbf{r})$ is now the macroscopic polarization field associated with the dielectric medium. Recalling Section 2.4.2, we may it write in the form of

$$\mathbf{P}(\mathbf{r}) = \int_0^\infty \mathrm{d}\omega\, \underline{\mathbf{P}}(\mathbf{r},\omega) + \text{c.c.}, \tag{10.90}$$

where

$$\underline{\mathbf{P}}(\mathbf{r},\omega) = \varepsilon_0[\varepsilon(\mathbf{r},\omega) - 1]\underline{\mathbf{E}}(\mathbf{r},\omega) + \underline{\mathbf{P}}_\mathrm{N}(\mathbf{r},\omega). \tag{10.91}$$

Inserting Eqs (10.61) and (10.62) into Eq. (10.59) and making use of Eq. (2.2), we find that the Lorentz force density can be rewritten as

$$\mathbf{f}_\mathrm{L}(\mathbf{r}) = \boldsymbol{\nabla}' \otimes \mathbf{P}(\mathbf{r})\mathbf{E}(\mathbf{r}')\big|_{\mathbf{r}'=\mathbf{r}} + \frac{\partial[\mathbf{P}(\mathbf{r}) \times \mathbf{B}(\mathbf{r})]}{\partial t} + \boldsymbol{\nabla}[\mathbf{P}(\mathbf{r}) \otimes \mathbf{E}(\mathbf{r})] \tag{10.92}$$

($\boldsymbol{\nabla}' \mathrel{\widehat{=}} \partial/\partial x_k'$). Hence the total Lorentz force acting on the matter which fills some space region of volume V, Eq. (10.60), can be represented in the form

$$\mathbf{F} = \int_V \mathrm{d}^3 r\, \boldsymbol{\nabla}' \otimes \mathbf{P}(\mathbf{r})\mathbf{E}(\mathbf{r}')\big|_{\mathbf{r}'=\mathbf{r}} + \frac{\mathrm{d}}{\mathrm{d}t}\int_V \mathrm{d}^3 r\, \mathbf{P}(\mathbf{r}) \times \mathbf{B}(\mathbf{r}) + \int_{\partial V} \mathrm{d}\mathbf{a}\mathbf{P}(\mathbf{r}) \otimes \mathbf{E}(\mathbf{r}). \tag{10.93}$$

In particular in the case of a body which is not embedded in a medium the surface integral taken with respect to the "outer" values of the integrand vanishes and Eq. (10.93) simplifies to

$$\mathbf{F} = \int_V \mathrm{d}^3 r\, \boldsymbol{\nabla}' \otimes \mathbf{P}(\mathbf{r})\mathbf{E}(\mathbf{r}')\big|_{\mathbf{r}'=\mathbf{r}} + \frac{\mathrm{d}}{\mathrm{d}t}\int_V \mathrm{d}^3 r\, \mathbf{P}(\mathbf{r}) \times \mathbf{B}(\mathbf{r}), \tag{10.94}$$

19) For an extension to magnetodielectric bodies, see Raabe and Welsch (2005).

which corresponds to the single-atom equation (10.64). Note that for $\mathbf{P}(\mathbf{r})$ from Eq. (10.63), Eq. (10.94) reduces to Eq. (10.64).

Equivalently, by recalling the local momentum balance as given by Eq. (2.7), we see that the total Lorentz force (acting on the matter in a space region of volume V) can be expressed in terms of the electric and induction fields as

$$\mathbf{F} = \int_{\partial V} \mathrm{d}\mathbf{a}\, \boldsymbol{T}(\mathbf{r}) - \varepsilon_0 \frac{\mathrm{d}}{\mathrm{d}t} \int_V \mathrm{d}^3 r\, \mathbf{E}(\mathbf{r}) \times \mathbf{B}(\mathbf{r}), \tag{10.95}$$

where $\boldsymbol{T}(\mathbf{r})$ is the ordinary stress tensor as given by Eq. (2.11), i. e.,

$$\boldsymbol{T}(\mathbf{r}) = \varepsilon_0 \mathbf{E}(\mathbf{r}) \otimes \mathbf{E}(\mathbf{r}) + \mu_0^{-1} \mathbf{B}(\mathbf{r}) \otimes \mathbf{B}(\mathbf{r}) - \tfrac{1}{2}[\varepsilon_0 \mathbf{E}^2(\mathbf{r}) + \mu_0^{-1} \mathbf{B}^2(\mathbf{r})]\boldsymbol{I}. \tag{10.96}$$

If the volume integral on the right-hand side of Eq. (10.95) can be regarded as being time-independent, then the total force is solely determined by the surface integral

$$\mathbf{F} = \int_{\partial V} \mathrm{d}\mathbf{F}, \tag{10.97}$$

where

$$\mathrm{d}\mathbf{F} = \mathrm{d}\mathbf{a}\, \boldsymbol{T}(\mathbf{r}) = \boldsymbol{T}(\mathbf{r})\, \mathrm{d}\mathbf{a} \tag{10.98}$$

can be regarded as the infinitesimal force element acting on the infinitesimal surface element $\mathrm{d}\mathbf{a}$.

Equation (10.93) [or (10.94)] and the equivalent equation (10.95) [together with Eq. (10.96)] are respectively basic formulas for calculating radiation forces on macroscopic bodies. Note that Eq. (10.95) is more general than Eq. (10.93), because it is also valid for other materials than dielectrics. The formulas can be analogously used in quantum theory as well, by regarding them as operator-valued ones and taking the expectation values. Recall that the noise polarization $\underline{\hat{\mathbf{P}}}_{\mathrm{N}}(\mathbf{r}, \omega)$ is given by Eq. (2.210). In particular, Eq. (10.94) then reads

$$\mathbf{F} = \int_V \mathrm{d}^3 r\, \boldsymbol{\nabla}' \langle \hat{\mathbf{P}}(\mathbf{r}) \hat{\mathbf{E}}(\mathbf{r}') \rangle \big|_{\mathbf{r}'=\mathbf{r}} + \frac{\mathrm{d}}{\mathrm{d}t} \int_V \mathrm{d}^3 r\, \langle \hat{\mathbf{P}}(\mathbf{r}) \times \hat{\mathbf{B}}(\mathbf{r}) \rangle, \tag{10.99}$$

which obviously corresponds to the single-atom equation (10.65). In a steady-state regime the second term on the right-hand side in this equation vanishes and the force formula reduces to

$$\mathbf{F} = \int_V \mathrm{d}^3 r\, \boldsymbol{\nabla}' \langle \hat{\mathbf{P}}(\mathbf{r}) \hat{\mathbf{E}}(\mathbf{r}') \rangle \big|_{\mathbf{r}'=\mathbf{r}'} \tag{10.100}$$

which corresponds to Eq. (10.66).

To calculate the Casimir force as the ground-state Lorentz force, we follow the line suggested by classical electrodynamics to derive Eq. (10.97) together

with Eqs (10.98) and (10.96), noting that the (expectation value of the) second term on the right-hand side in Eq. (10.95) vanishes. Hence

$$\mathbf{F} = \int_{\partial V} \mathrm{d}\mathbf{a}\, \boldsymbol{T}(\mathbf{r}), \tag{10.101}$$

where the (time-independent) Casimir stress tensor $\boldsymbol{T}(\mathbf{r})$ can be obtained, in agreement with the classical equation (10.96), from the quantum-mechanical ground-state expectation value

$$\begin{aligned}\boldsymbol{T}(\mathbf{r},\mathbf{r}') = {} & \varepsilon_0 \langle\{0\}|\hat{\mathbf{E}}(\mathbf{r}) \otimes \hat{\mathbf{E}}(\mathbf{r}')|\{0\}\rangle + \mu_0^{-1}\langle\{0\}|\hat{\mathbf{B}}(\mathbf{r}) \otimes \hat{\mathbf{B}}(\mathbf{r}')|\{0\}\rangle \\ & - \tfrac{1}{2}\boldsymbol{I}\left[\varepsilon_0 \langle\{0\}|\hat{\mathbf{E}}(\mathbf{r})\hat{\mathbf{E}}(\mathbf{r}')|\{0\}\rangle + \mu_0^{-1}\langle\{0\}|\hat{\mathbf{B}}(\mathbf{r})\hat{\mathbf{B}}(\mathbf{r}')|\{0\}\rangle\right]\end{aligned} \tag{10.102}$$

in the coincidence limit,

$$\boldsymbol{T}(\mathbf{r}) = \lim_{\mathbf{r}'\to\mathbf{r}} \boldsymbol{T}(\mathbf{r},\mathbf{r}'), \tag{10.103}$$

where divergent bulk contributions are to be removed before taking the limit. This is always possible if the body under study is embedded in a material environment which is homogeneous at least in the vicinity of the body. If this is not the case, special care and additional considerations may be necessary. Note that in the calculation of the surface integral in Eq. (10.101) the "outer" values of the integrand should be used if ∂V is the interface between an inhomogeneous body and a near-surface homogeneous medium in which the body is embedded.

Recalling the commutation relations (2.208) and (2.209) and making use of the field representation as given by Eqs (2.211)–(2.214), we can calculate the field correlation functions in Eq. (10.102) in a straightforward way. By means of the commutation relations (2.208) and (2.209) it is not difficult to see that [recall Eq. (10.7)]

$$\langle\{0\}|\hat{\mathbf{f}}(\mathbf{r},\omega) \otimes \hat{\mathbf{f}}^\dagger(\mathbf{r}',\omega')|\{0\}\rangle = \delta(\omega-\omega')\delta(\mathbf{r}-\mathbf{r}'), \tag{10.104}$$

$$\langle\{0\}|\hat{\mathbf{f}}(\mathbf{r},\omega) \otimes \hat{\mathbf{f}}(\mathbf{r}',\omega')|\{0\}\rangle = 0. \tag{10.105}$$

Using Eqs (2.211)–(2.214), together with Eqs (10.104) and (10.105), we then derive, on employing the relation (A.3),

$$\langle\{0\}|\hat{\mathbf{E}}(\mathbf{r}) \otimes \hat{\mathbf{E}}(\mathbf{r}')|\{0\}\rangle = \frac{\hbar\mu_0}{\pi}\int_0^\infty \mathrm{d}\omega\, \omega^2 \mathrm{Im}\, \boldsymbol{G}(\mathbf{r},\mathbf{r}',\omega), \tag{10.106}$$

$$\langle\{0\}|\hat{\mathbf{B}}(\mathbf{r}) \otimes \hat{\mathbf{B}}(\mathbf{r}')|\{0\}\rangle = -\frac{\hbar\mu_0}{\pi}\int_0^\infty \mathrm{d}\omega\, \boldsymbol{\nabla} \times \mathrm{Im}\, \boldsymbol{G}(\mathbf{r},\mathbf{r}',\omega) \times \underleftarrow{\boldsymbol{\nabla}}'. \tag{10.107}$$

Combination of Eqs (10.102), (10.106) and (10.107) eventually yields

$$\boldsymbol{T}(\mathbf{r},\mathbf{r}') = \boldsymbol{\theta}(\mathbf{r},\mathbf{r}') - \tfrac{1}{2}\boldsymbol{I}\,\mathrm{Tr}\,\boldsymbol{\theta}(\mathbf{r},\mathbf{r}'), \tag{10.108}$$

where

$$\boldsymbol{\theta}(\mathbf{r},\mathbf{r}') = \frac{\hbar}{\pi}\int_0^\infty \mathrm{d}\omega\,\left[\frac{\omega^2}{c^2}\,\mathrm{Im}\,\boldsymbol{G}(\mathbf{r},\mathbf{r}',\omega) - \boldsymbol{\nabla}\times\mathrm{Im}\,\boldsymbol{G}(\mathbf{r},\mathrm{r}',\omega)\times\underleftarrow{\boldsymbol{\nabla}}'\right]. \quad (10.109)$$

Note that the permittivity $\varepsilon(\mathbf{r},\omega)$ does not appear explicitly in Eq. (10.109), but only via the Green tensor $\boldsymbol{G}(\mathbf{r},\mathbf{r}',\omega)$.[20] Having removed divergent bulk contributions [by replacing the Green tensor $\boldsymbol{G}(\mathbf{r},\mathbf{r}',\omega)$ with its scattering part $\boldsymbol{G}_\mathrm{S}(\mathbf{r},\mathbf{r}',\omega)$, cf. Eq. (10.30)], we may take the imaginary part of the whole integral instead of the integrand in Eq. (10.109) and rotate the integration contour in the usual way toward the imaginary frequency axis, on which the Green tensor is real. In this way we arrive at

$$\boldsymbol{T}(\mathbf{r}) = \boldsymbol{\theta}_\mathrm{S}(\mathbf{r}) - \tfrac{1}{2}\boldsymbol{I}\,\mathrm{Tr}\,\boldsymbol{\theta}_\mathrm{S}(\mathbf{r}), \quad (10.110)$$

where

$$\boldsymbol{\theta}_\mathrm{S}(\mathbf{r}) = -\frac{\hbar}{\pi}\int_0^\infty \mathrm{d}u\,\left[\frac{u^2}{c^2}\,\boldsymbol{G}_\mathrm{S}(\mathbf{r},\mathbf{r},iu) + \boldsymbol{\nabla}\times\boldsymbol{G}_\mathrm{S}(\mathbf{r},\mathbf{r},iu)\times\underleftarrow{\boldsymbol{\nabla}}'\right]. \quad (10.111)$$

Now we insert Eq. (10.110) into Eq. (10.101) to obtain the following expression for the Casimir force:

$$\mathbf{F} = \int_{\partial V}\mathrm{d}\mathbf{a}\left[\boldsymbol{\theta}_\mathrm{S}(\mathbf{r}) - \tfrac{1}{2}\boldsymbol{I}\,\mathrm{Tr}\,\boldsymbol{\theta}_\mathrm{S}(\mathbf{r})\right]. \quad (10.112)$$

10.2.2.2 Planar structures

Let us apply the theory to a planar dielectric structure defined according to

$$\varepsilon(\mathbf{r},\omega) = \begin{cases} \varepsilon_-(z,\omega) & z<0,\\ \varepsilon(\omega) & 0<z<d,\\ \varepsilon_+(z,\omega) & z>d \end{cases} \quad (10.113)$$

(Fig. 10.7). To determine the Casimir stress in the interspace $0<z<d$, we need, according to Eqs (10.110) and (10.111), the (scattering part of the) Green tensor for both spatial arguments within the interspace ($0<z=z'<d$). As in the example studied in Section 10.2.1.2, the calculation can be performed on the basis of the well-known Green tensor for a multi-layer dielectric structure of infinite lateral extension. We again renounce the rather lengthy but straightforward calculation and present the final result. For symmetry reasons it is clear that the stress tensor effectively reduces to the T_{zz} component, which can be given in the form of [Raabe and Welsch (2005)]

$$T_{zz}(z) = -\frac{\hbar}{8\pi^2}\int_0^\infty \mathrm{d}u\int_0^\infty \mathrm{d}q\,\frac{q}{\kappa(iu,q)}\,g(z,iu,q), \quad (10.114)$$

20) Equation (10.109) is also valid for magnetodielectrics, if $\boldsymbol{G}(\mathbf{r},\mathbf{r}',\omega)$ is understood as the Green tensor of the inhomogeneous Helmholtz equation with $\varepsilon(\mathbf{r},\omega)$ and $\mu(\mathbf{r},\omega)$ [Raabe and Welsch (2005)].

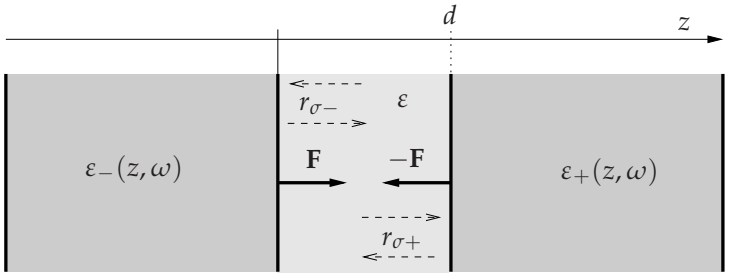

Fig. 10.7 Two (multi-layer) dielectric plates are subject to a mutual attractive force, whose absolute value (per unit area) $F=T_{zz}(d)$, Eq. (10.114), is, for chosen spacing d, determined by the coefficients of (virtual-)photon reflection $r_{\sigma-}$ ($r_{\sigma+}$) at the left (right) plate ($\sigma=s,p$).

where

$$\kappa(iu,q)=\sqrt{q^2-\varepsilon(iu)\,\frac{(iu)^2}{c^2}} \tag{10.115}$$

and

$$\begin{aligned} g(z,iu,q) = &-2[\kappa^2(1+\varepsilon^{-1})+q^2(1-\varepsilon^{-1})]D_s^{-1}r_{s+}r_{s-}e^{-2\kappa d}\\ &-2[\kappa^2(1+\varepsilon^{-1})-q^2(1-\varepsilon^{-1})]D_p^{-1}r_{p+}r_{p-}e^{-2\kappa d}\\ &+(\kappa^2-q^2)(1-\varepsilon^{-1})D_s^{-1}\left[r_{s-}e^{-2\kappa z}+r_{s+}e^{-2\kappa(d-z)}\right]\\ &-(\kappa^2-q^2)(1-\varepsilon^{-1})D_p^{-1}\left[r_{p-}e^{-2\kappa z}+r_{p+}e^{-2\kappa(d-z)}\right] \end{aligned} \tag{10.116}$$

with

$$D_\sigma=D_\sigma(iu,q)=1-r_{\sigma+}r_{\sigma-}e^{-2\kappa d} \tag{10.117}$$

[$r_{\sigma\pm}$ are the reflection coefficients referring to reflection of waves at the right (+) and left (−) wall, as seen from the interspace, cf. Fig. 10.7]. Note that in Eqs (10.116) and (10.117) $\varepsilon=\varepsilon(iu)$, $\kappa=\kappa(iu,q)$, and $r_{\sigma\pm}=r_{\sigma\pm}(iu,q)$.

To further (numerically) evaluate Eq. (10.114), knowledge of the dependence of the reflection coefficients on u and q is required. Let us here restrict our attention to (i) the retarded limit and (ii) the limit of perfectly reflecting plates. That is to say, we (i) assume that the distance d between the plates is not too small so that the permittivities can be replaced by their static values, and (ii) we set

$$r_{p\pm}=-r_{s\pm}=1. \tag{10.118}$$

It is then not difficult to calculate the simplified integrals in Eq. (10.114) analytically to obtain the Casimir force per unit area as [$\varepsilon\equiv\varepsilon(0)$]

$$F=T_{zz}(d)=\frac{\hbar c\pi^2}{240}\frac{1}{\sqrt{\varepsilon}}\left(\frac{2}{3}+\frac{1}{3\varepsilon}\right)\frac{1}{d^4}\,, \tag{10.119}$$

which reduces to Casimir's and Polder's famous formula

$$F = \frac{\hbar c \pi^2}{240} \frac{1}{d^4} \tag{10.120}$$

[Casimir and Polder (1948)] in the case when the interspace between the plates is empty ($\varepsilon = 1$).

References

Bethe, H.A. (1947) *Phys. Rev.* **72**, 339.

Buhmann, S.Y, L. Knöll, D.-G. Welsch and T.D. Ho (2004) *Phys. Rev. A* **70**, 052117.

Buhmann, S.Y and D.-G. Welsch (2006) *Appl. Phys. B* **82**, 189.

Casimir, H.B.G. and D. Polder (1948) *Phys. Rev.* **73**, 360.

Chew, W.C. (1995) *Waves and Fields in Inhomogeneous Media* (IEEE Press, New York).

Drexhage, K.H. (1974) in *Progress in Optics*, Vol. XXII, ed. E. Wolf (Elsevier, Amsterdam), p. 165.

Fain, V.M. and Ya.I. Khanin (1969) *Quantum Electronics* (MIT Press, Cambridge MA).

Feinberg, G. and J. Sucher (1970) *Phys. Rev. A* **2**, 2395 (1970).

Henkel, C. and V. Sandoghdar (1998) *Opt. Commun.* **158**, 250.

Ho, T.D, L. Knöll and D.-G.Welsch (2000) *Phys. Rev. A* **62**, 053804.

Ho, T.D, L. Knöll and D.-G.Welsch (2001) *Phys. Rev. A* **64**, 013804.

Ho, T.D., S.Y. Buhmann, L.Knöll, D.-G. Welsch, S. Scheel and J.Kästel (2003) *Phys. Rev. A* **68**, 043816.

Kleppner, D. (1981) *Phys. Rev. Lett.* **47**, 233.

Lamb, W.E. and R.C. Retherford (1947) *Phys. Rev.* **72**, 241.

Lennard-Jones, J.E. (1932) *Trans. Farad. Soc.* **28**, 333.

London, F. (1930) *Z. Physik* **63**, 245.

Milonni, P.W. (1994) *The Quantum Vacuum* (Academic Press, San Diego).

Purcell, E.M. (1946) *Phys. Rev.* **69**, 681.

Raabe, C. and D.-G. Welsch (2005) *Phys. Rev. A* **71**, 013814.

Sandoghdar, V., C.I. Sukenik, E.A. Hinds and S. Haroche (1992) *Phys. Rev. Lett.* **68**, 3432.

Tai, C.-T. (1994) *Dyadic Green Functions in Electromagnetic Theory* (IEEE Press, New York).

Tomaš, M.S. (1995) *Phys. Rev. A* **51**, 2545.

Verwey, E.J.W. and J.T.G. Overbeek (1948) *Theory of the Stability of Lyophobic Colloids* (Elsevier, Amsterdam).

Weisskopf, V. and E. Wigner (1930) *Z. Phys.* **63**, 54.

Yeung, M.S. and T.K. Gustafson (1996) *Phys. Rev. A* **54**, 5227.